QUALIFYING A HIGH PURITY GERMANIUM DETECTOR

by

Kylee Thomas

A senior thesis submitted to the faculty of

Brigham Young University - Idaho

in partial fulfillment of the requirements for the degree of

Bachelor of Science

Department of Physics

Brigham Young University - Idaho

December 2025

BRIGHAM YOUNG UNIVERSITY - IDAHO

DEPARTMENT APPROVAL

of a senior thesis submitted by

Kylee Thomas

This thesis has been reviewed by the research committee, senior thesis coordinator, and department chair and has been found to be satisfactory.

Date	Evan Hansen, Chair, Advisor
Date	David Oliphant, Senior Thesis Coordinator
Date	Richard Datwyler, Committee Member
Date	Todd Lines, Committee Member

ABSTRACT

QUALIFYING A HIGH PURITY GERMANIUM DETECTOR

Kylee Thomas

Department of Physics

Bachelor of Science

This thesis presents the preparation and qualification of a Mirion Canberra High Purity Germanium (HPGe) detector for use in positron annihilation spectroscopy (PAS) at Brigham Young University–Idaho. The system was set up and calibrated using standard gamma-ray sources, and its energy resolution was verified with full width at half maximum measurements, achieving 0.60 keV at 122 keV and 1.62 keV at 1332 keV, satisfying manufacturer specifications. Using the detector, S parameters were calculated from positron annihilation spectra using a Na-22 isotope and various sample materials. A linear correlation between S parameters of the same materials measured with this detector and an Ortec HPGe detector confirmed cross-system consistency. These results verify the detector's suitability for high-precision PAS experiments and establish a foundation for future coincidence Doppler broadening and other material structure studies.

ACKNOWLEDGMENTS

Firstly, I thank my sweet husband, Ethan. I would not have stayed sane through this whole process if it weren't for you. Thank you for your encouragement and for always believing in me.

I would like to express my sincere gratitude to Dr. Evan Hansen, who served as both my project advisor and senior thesis advisor. His guidance, enthusiasm, and range of knowledge in positron annihilation spectroscopy were so helpful throughout every stage of this work. His support and encouragement were essential to the successful completion of this thesis.

I would also like to thank George Evans, alumnus of the PAS research group and current researcher at Idaho National Laboratory, for his continued mentorship and technical guidance. His expertise and experience in positron annihilation spectroscopy, along with his willingness to share real-world experience and insight, greatly strengthened both this project and my understanding of the field.

Finally, I would like to acknowledge the support of the Department of Physics at Brigham Young University–Idaho for providing the resources, facilities, and academic environment that made this research possible.

Contents

Table of Contents **xi**

List of Figures **xiii**

1 Introduction **1**
1.1 Background and Motivation 1
1.2 Doppler Broadening of Positron-Electron Annihilation Gamma Rays . 3
1.3 Functions of High Purity Germanium Detectors and Data Acquisition 6

2 Methods and Challenges **11**
2.1 Detector Setup and Important Specifications 11
2.2 Pulse Height Analysis and Calibration 12
2.3 Processing the Data and Calculating the S Parameter 14
2.4 Detector Compatibility and Optimization 17

3 Results and Conclusions **19**
3.1 Detector Qualification and Verified Results 19
3.2 Criteria for Detector Qualification and Analysis Reliability 20
3.3 Future Research and Applications 21

Bibliography **23**

List of Figures

1.1 The effects of vacancies on the Sharpness Parameter [1] 3
1.2 Example Doppler-Broadened curve along with highlighted S and W Parameter bounds and labeled background. Plot created by university's analysis program PAPPy. 4
1.3 Example of annealing structure migrating back into lattice structure (created by Emma Andersen) 4
1.4 S Parameters before and after annealing six different metals. Measured by university PAS research team in Spring 2023. 5
1.5 Full Width Half Max line at the mid-point of the centroid line for this energy peak. 6
1.6 Close up of semiconductor crystal part of university's model of Mirion HPGe detector, particularly the Broad Energy Ge detector [2]. 7
1.7 Analog to Digital Converter (top) and Energy Converted Pulse (bottom). A sharp pulse proportional to the energy is created when a gamma ray comes in contact with the crystal and then converted into a trapezoidal energy peak. 8
1.8 Isotope peaks as measured by ProSpect for barium-133 and cesium-137, and the Doppler-broadened peak from sodium-22. Plot is a histogram of Counts vs Energy in keV. 9
1.9 PAS measurement device setup. (Left to right) liquid nitrogen, Ortec HPGe detector, Mirion HPGe Detector, and Lynx Digital Signal Analyzer. 9

2.1 Screenshot of ProSpect calibration screen. The selected regions are assigned to their corresponding energy levels and the fit equation is found automatically. This is an example calibration and not the one used for measurements. 13
2.2 Doppler-broadened peak showing S Region and S Bounds (r_o and r_f), the Peak Region and bounds (P_o and P_f), the Lower Background (LB), and Upper Background (UB) [3]. 15
2.3 Doppler-broadened peak depicting the background line and indicating S Region and Peak Region (P_o and P_f), the Lower Background (L_o to L_f), and Upper Background (U_o to U_f) [3]. 16

2.4 Offset 511 keV peaks measured with the Ortec detector (centered) and Mirion (right). The program shows horizontal axis to be energy, while in actuality is based on channels. 17
2.5 Average S Parameters for each sample measured on each detector compared. Horizontal axis (S Parameters measured on the Ortec detector), vertical axis (S Parameters measured on the Mirion detector). A linear fit line is shown ($y = 0.66x + 0.10$). 18

3.1 S Parameters of the same sample untouched taken multiple times with each detector. Error bar size ranges from $4.97 \cdot 10^{-4}$ to $5.60 \cdot 10^{-4}$ . . 21

Chapter 1

Introduction

1.1 Background and Motivation

High-precision radiation detection plays a pivotal role in many modern scientific and engineering applications. Some of these include nuclear spectroscopy, medical imaging, environmental monitoring, and materials science. Radiation detection involves converting interactions of ionizing particles into measurable electrical signals. This can be used to determine the energy of the radiation. Accurate measurement of these signals helps researchers analyze materials and find defects in those materials, as well as study nuclear decay [4].

Traditionally, instruments such as Geiger–Müller tubes and scintillation detectors have been widely used for radiation measurement. These devices do not provide sufficient sensitivity, although they provide measurement across a wide range of energies. One analogy that could be appropriate would be looking at a picture from a far and not being able to see the finer details of it. It is still possible to distinguish between the gamma-ray emissions of barium-133 and cesium-137, however one would not be able to see the many individual peaks of barium-133 that are closely spaced.

Such limitations render scintillation-based systems less suitable for applications requiring high-resolution energy distinction. Thus, high resolution radiation detection is necessary in Doppler broadening studies of materials.

Semiconductor detectors overcome many of these limitations by directly converting photon energy into electron–hole pairs within a crystal lattice. Germanium detectors have excellent charge collection efficiency, resulting in extremely sharp spectral peaks and precise energy measurements. A High Purity Germanium (HPGe) detector can achieve energy resolutions as low as 5.9 keV with a resolution at most 0.4 keV wide vastly outperforming scintillation detectors [5] [2]. However, due to its narrow band gap, germanium must be operated at low temperatures using liquid nitrogen cooling. When properly cooled, an HPGe detector provides accurate, stable, and reproducible data for spectroscopy.

Recently, Brigham Young University Idaho acquired a new HPGe detection system from Mirion Technologies to support advanced positron annihilation spectroscopy (PAS) experiments. Upon receiving this detector, it was critical to validate its performance to ensure it met manufacturer specifications and the research group's expectations. Specifically, Mirion guarantees resolutions of $\leq$ 0.650 keV at 122 keV (cobalt-57) and $\leq$ 1.8 keV at 1332 keV (cobalt-60) [6]. This qualification ensures that future measurements reflect material behavior rather than electronic noise, improper calibration, or detector malfunction. This thesis documents the setup, calibration, and qualification of the new HPGe detector. This establishes a new step for PAS research at the university.

1.2 Doppler Broadening of Positron-Electron Annihilation Gamma Rays

Positron-electron annihilation spectroscopy is useful to probe for vacancies in solid materials. When a positron, the antiparticle of an electron, is sent into a solid, often using a sodium-22 isotope, it annihilates with an electron, producing two gamma rays of approximately 511 keV each. There is a Doppler broadening effect when the electron involved in the annihilation has momentum. This momentum is transferred to the emitted photons, which causes a measurable energy shift. By analyzing the energy distribution around 511 keV, researchers can infer information about the momentum distribution of the electrons. This information tells us about the presence of vacancies or defects in the lattice structure [3].

In an ideal, defect-free crystal, annihilation typically occurs with tightly bound valence electrons. This results in a narrow peak centered at 511 keV. In a sample with many vacancies, annihilation often involves less tightly bound electrons, thus lower state electrons are present, producing a broader energy distribution.

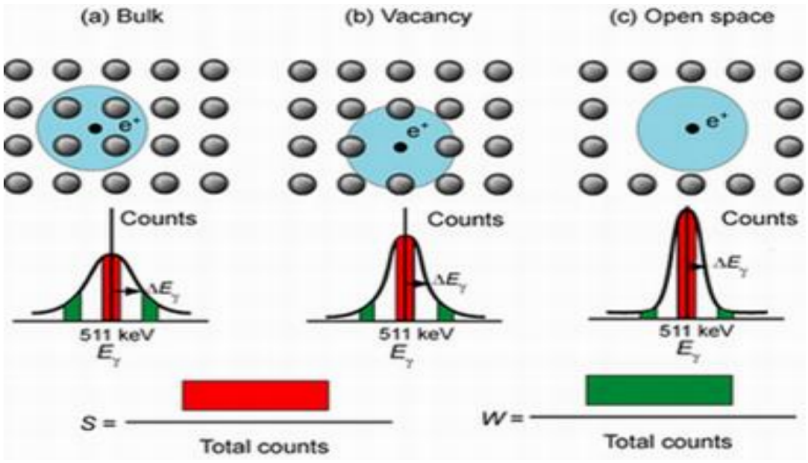

Figure 1.1 The effects of vacancies on the Sharpness Parameter [1]

This is why the width and shape of the Doppler-broadened peak provide insight

into the defect environment. This is often expressed using parameters such as the S parameter (sharpness) and W parameter (wing area), which characterize the central and outer regions of the energy spectrum [7].

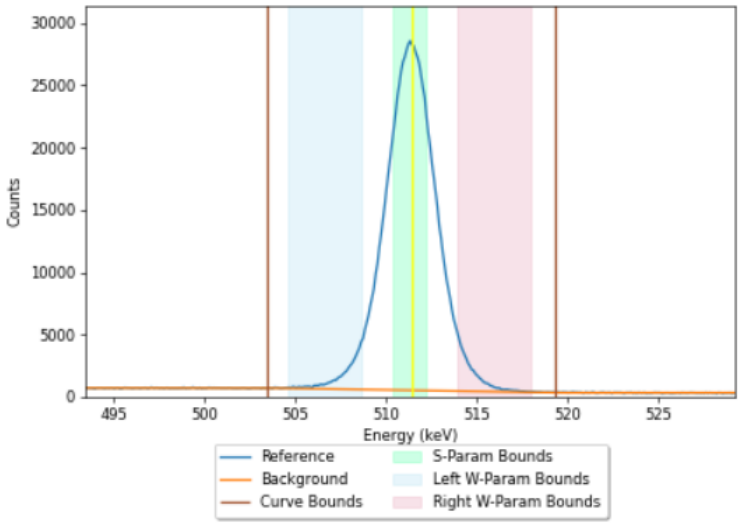

Figure 1.2 Example Doppler-Broadened curve along with highlighted S and W Parameter bounds and labeled background. Plot created by university's analysis program PAPPy.

A way to reduce defect concentration is called annealing. Annealing is a controlled heating process by heating up a metal to high temperatures and allowing it to cool slowly. This allows atoms to migrate back into lattice positions.

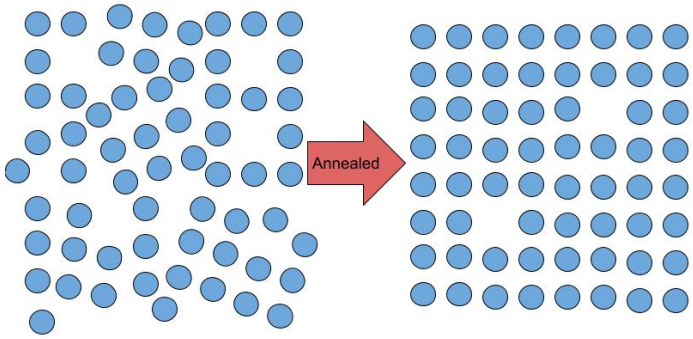

Figure 1.3 Example of annealing structure migrating back into lattice structure (created by Emma Andersen)

PAS studies compare pre- and post-annealed samples to quantify this recovery process. For instance, Taylor et al. (2021) observed that tungsten samples irradiated at 500 °C exhibited significantly more vacancy clusters than those irradiated at higher temperatures, demonstrating that temperature strongly influences defect filling [8]. In past university PAS research, we were able to reproduce these results by measuring S Parameters of six separate metals pre- and post-annealing and saw a significant change in this parameter showing a drop in sharpness after annealing.

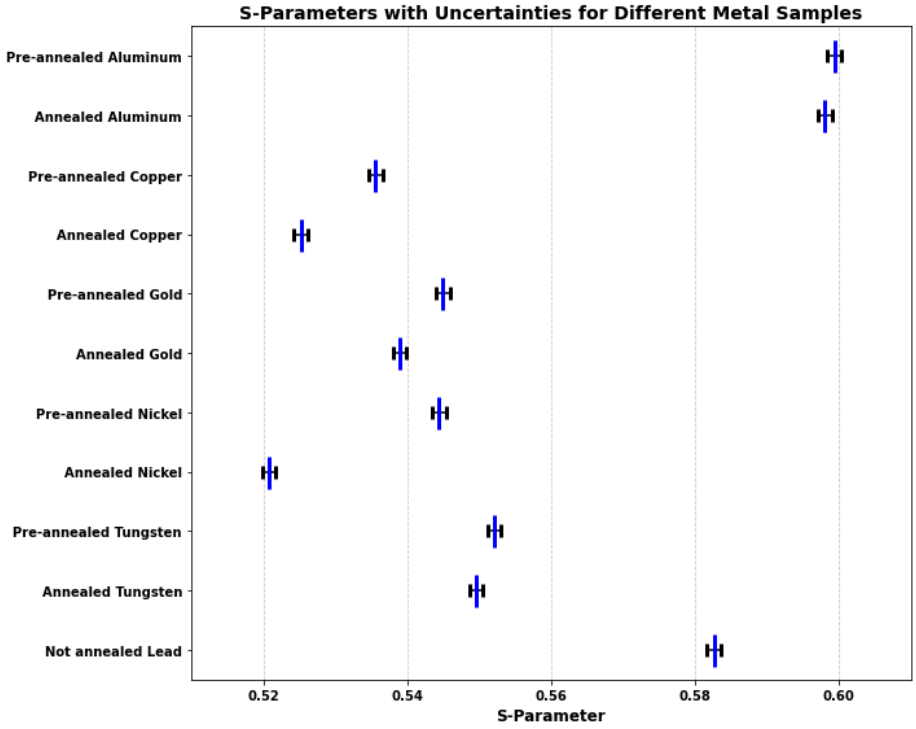

Figure 1.4 S Parameters before and after annealing six different metals. Measured by university PAS research team in Spring 2023.

Accurate Doppler broadening measurements, therefore, depend critically on detector resolution: a poorly resolved 511 keV peak could mask subtle defect-induced variations. This underscores the importance of verifying that the HPGe system meets its specified resolution measured in Full Width at Half Maximum (FWHM) before conducting experiments. FWHM shown in Figure 1.5 is as the name implies, the

width of a gaussian curve at half the maximum height at the centroid [4]. This curve is not always gaussian if there is not a sufficient amount of counts. There is extensive math involved in the calculation of the FWHM, however the ProSpect program has a built in computation to give this measurement for selected peaks.

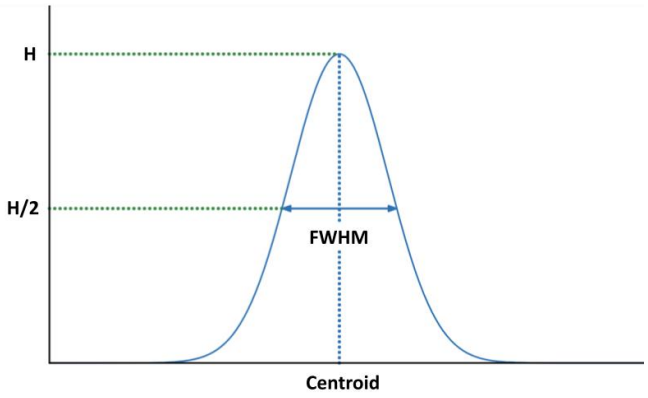

Figure 1.5 Full Width Half Max line at the mid-point of the centroid line for this energy peak.

1.3 Functions of High Purity Germanium Detectors and Data Acquisition

An HPGe detector operates by using the semiconducting properties of germanium to convert incident gamma-ray energy into measurable electrical signals. The detector crystal is typically a few centimeters in diameter and thickness. The crystal is doped to create p-type and n-type regions. When a gamma ray interacts with the crystal, it generates electron–hole pairs proportional to the photon energy.

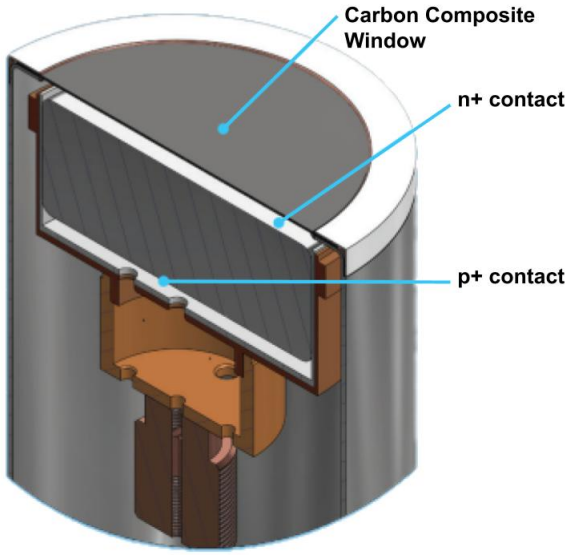

Figure 1.6 Close up of semiconductor crystal part of university's model of Mirion HPGe detector, particularly the Broad Energy Ge detector [2].

The resulting charge pulse is collected by electrodes and converted into a voltage signal via a charge-sensitive preamplifier. In this experiment, the detector's output is fed into a Lynx digital signal analyzer. This digitizes the signal for processing by the ProSpect spectroscopy software program [9]. Within ProSpect, shaping times, rise times, flat-top times, and gain can be adjusted to optimize resolution. Proper electronic pulse shaping minimizes noise while maintaining adequate measurement. For the Mirion HPGe system, typical shaping parameters are 10.8 μs rise time and 2.0 μs flat top [6].

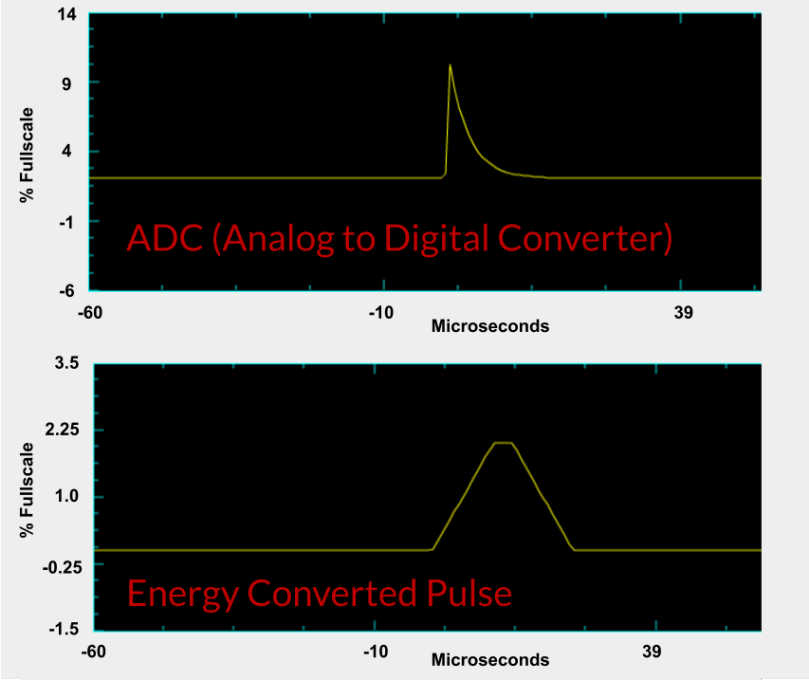

Figure 1.7 Analog to Digital Converter (top) and Energy Converted Pulse (bottom). A sharp pulse proportional to the energy is created when a gamma ray comes in contact with the crystal and then converted into a trapezoidal energy peak.

ProSpect then generates histograms of energy versus counts (Figure 1.8), producing the familiar gamma-ray spectra. By calibrating the energy scale using standard isotopes such as cesium-137, cobalt-60, and barium-133, each channel can be mapped to a specific range of energy.

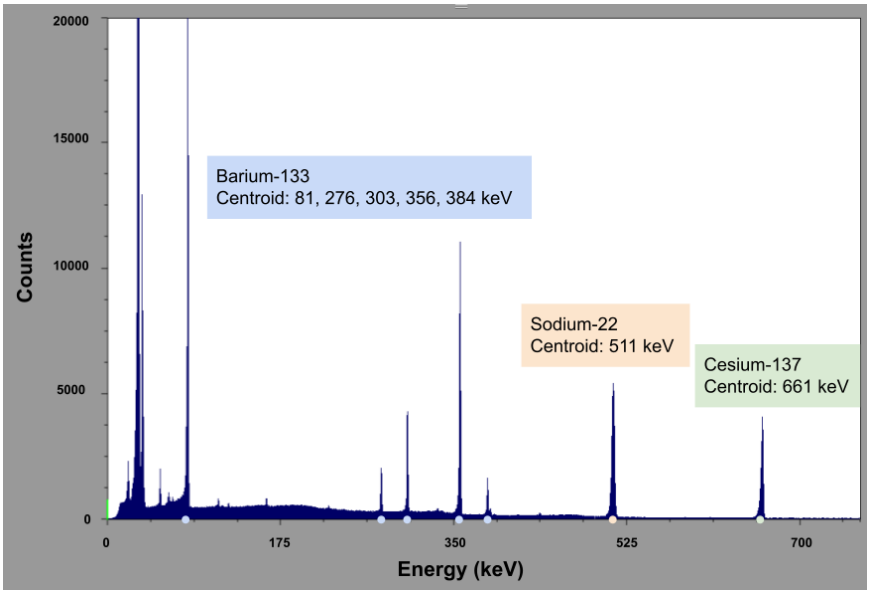

Figure 1.8 Isotope peaks as measured by ProSpect for barium-133 and cesium-137, and the Doppler-broadened peak from sodium-22. Plot is a histogram of Counts vs Energy in keV.

This allows researchers to extract quantitative parameters such as the Full Width Half Max (FWHM) and S parameter for analysis of Doppler broadening and material defects. The combination of HPGe detector, Lynx digital signal analyzer, and ProSpect software make the full system necessary for advanced PAS experiments.

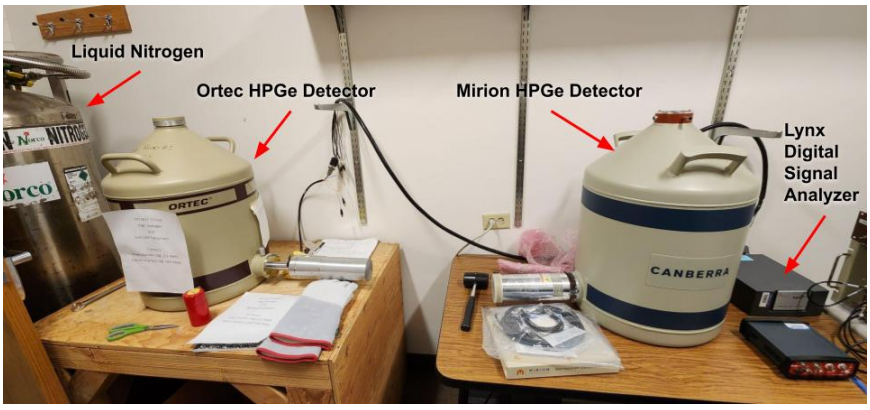

Figure 1.9 PAS measurement device setup. (Left to right) liquid nitrogen, Ortec HPGe detector, Mirion HPGe Detector, and Lynx Digital Signal Analyzer.

Chapter 2

Methods and Challenges

2.1 Detector Setup and Important Specifications

Before performing any positron-annihilation measurements, it was necessary to verify that the newly installed Mirion Canberra HPGe detector performed according to its specified characteristics. The detector was integrated with a Mirion Lynx digital signal analyzer and controlled via the ProSpect gamma spectroscopy software package [9]. The Lynx unit provided programmable shaping, gain, and filtering options and digitizing the pulse output from the detector preamplifier. The entire assembly was cooled with liquid nitrogen to maintain the germanium crystal near 77 K.

The most critical performance parameter for gamma spectroscopy is energy resolution, calculated by finding the FWHM of a reference gamma-ray peak. The manufacturer guarantees resolutions of ≤ 0.650 keV at 122 keV (cobalt-57) and ≤ 1.800 keV at 1332 keV (cobalt-60) under standard conditions [6]. Achieving these values requires correct setup of electronic shaping times, flat-top widths, and pole-zero compensation. Improper settings or offset in calibration can cause pulse pile-up and degraded resolution.

Several test spectra were collected from standard sources, including ^{57}Co, ^{60}Co, and ^{137}Cs, to assess performance. Initial results previously showed low resolution due to a calibration error in the pulse shaping filter. After recalibration, the measured FWHM values were:

$$FWHM(122 \text{ keV}) = 0.60 \pm 0.0 \text{ keV}$$

$$FWHM(1332 \text{ keV}) = 1.62 \pm 0.02 \text{ keV}$$

which meet Mirion's specifications. These results confirm that the detector operates within given performance limits, qualifying it for Doppler broadening analysis.

2.2 Pulse Height Analysis and Calibration

Each gamma-ray interaction within the detector crystal produces a pulse whose amplitude is proportional to the deposited energy. The pulse height analyzer (PHA) within the Lynx digitizes these signals, assigning them to discrete "channels" that represent small energy bins. The distribution of counts versus channel number thus forms the gamma spectrum. Several electronic parameters influence this process, including gain polarity, shaping time, rise time, flat top, and dead time correction. [9]

Calibration is essential to translate channel numbers into physical energy units (keV). This was accomplished using multiple calibration sources with well-known peak energies:

- ^{57}Co (122 keV and 136 keV)
- ^{137}Cs (662 keV)
- ^{60}Co (1173 keV and 1332 keV)
- ^{133}Ba (80-383 keV region)

A linear relationship of the form

$$\text{"Energy"} = m \cdot \text{"Channel"} + b$$

was fitted between channel and energy, where m is the energy-per-channel scaling factor and b is the zero-offset. Two or more calibration points were sufficient to determine these constants, though including additional peaks (from barium and cesium) improved fit accuracy across the full energy range.

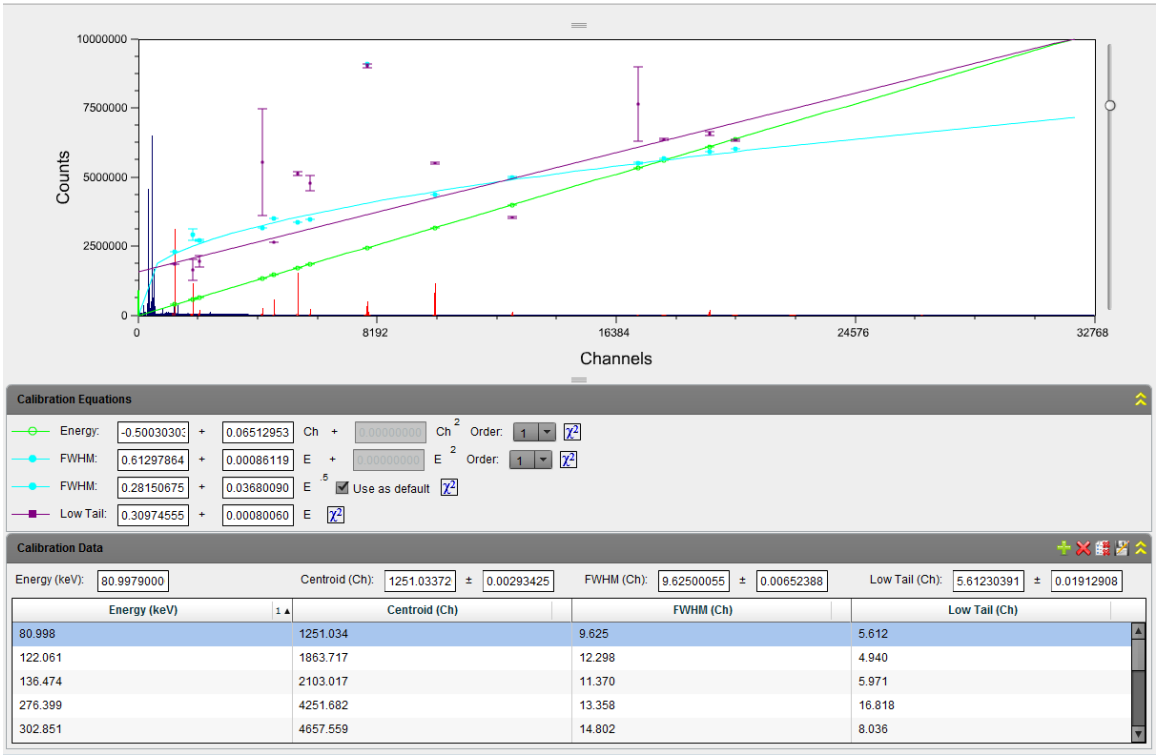

Figure 2.1 Screenshot of ProSpect calibration screen. The selected regions are assigned to their corresponding energy levels and the fit equation is found automatically. This is an example calibration and not the one used for measurements.

The detector coarse gain was initially adjusted such that the 511 keV annihilation peak fell near the midpoint of the spectrum window (about 8192 channels). However, the cobalt-60 peak at 1332 keV used for the resolution specifications was not visible in the spectrum window until the coarse gain was turned to 32768 channels. This

ensured that both the low-energy and high-energy sides of the Doppler-broadened peak were well represented within the histogram. This coarse gain may not be ideal, since the energy levels of interest were squeezed to the lower end of the window.

During calibration, shaping parameters were optimized to minimize FWHM. The manufacturer's suggested values of 10.8 μs rise time and 2.0 μs flat top were used as starting points. Adjustments of ± 0.2 μs were tested to balance resolution, confirming that the default values are optimal.

2.3 Processing the Data and Calculating the S Parameter

After acquisition, the ProSpect software exports histograms of counts per energy bin. These were analyzed to quantify the sharpness and width of the 511 keV annihilation peak. The central measure used in Doppler broadening studies is the S parameter, representing the fraction of counts in the central portion of the peak relative to the total counts across the full energy window. The S parameter provides a quantitative measure of how "sharp" the annihilation peak is. Narrower peaks (higher S) correspond to annihilations with low-momentum electrons, typical of vacancies, while broader peaks (lower S) indicate interactions with higher momentum electrons [3, 7].

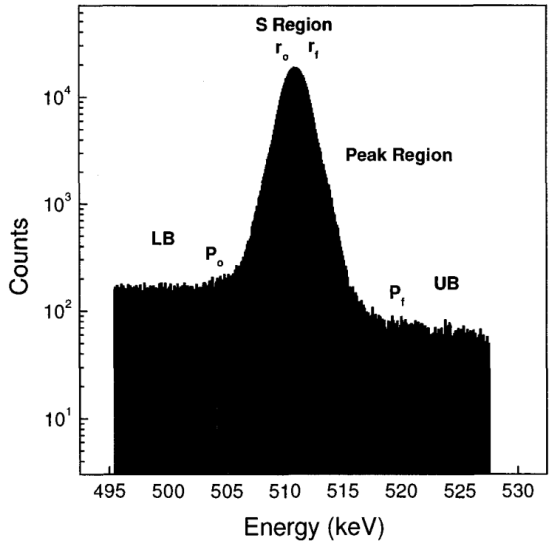

Figure 2.2 Doppler-broadened peak showing S Region and S Bounds (r_o and r_f), the Peak Region and bounds (P_o and P_f), the Lower Background (LB), and Upper Background (UB) [3].

Following Gagliardi (2008), the S parameter is defined as

$$S = \frac{\sum_{i=r_o}^{r_f} y_i - b_l - \frac{b_u - b_l}{P_f - P_o}(i - P_o)}{\sum_{i=P_o}^{P_f} y_i - b_l - \frac{b_u - b_l}{P_f - P_o}(i - P_o)}$$

where y_i number of counts at channel i, P_f and P_o are the upper and lower peak bounds respectively, r_f and r_o are the upper and lower S bound, and b_u and b_l are the upper and lower background measured at P_f and P_o respectively by

$$b_l = \frac{1}{Lf - L_o + 1} \sum_{i=L_o}^{L_f} y_i$$

$$b_u = \frac{1}{Uf - U_o + 1} \sum_{i=U_o}^{U_f} y_i$$

.

The numerator represents the narrow central area of the annihilation peak, otherwise know as the S Region, and the denominator represents the total area inside the

peak. Both have the background removed to account for only the annihilation within the sample as depicted in Figure 2.3.

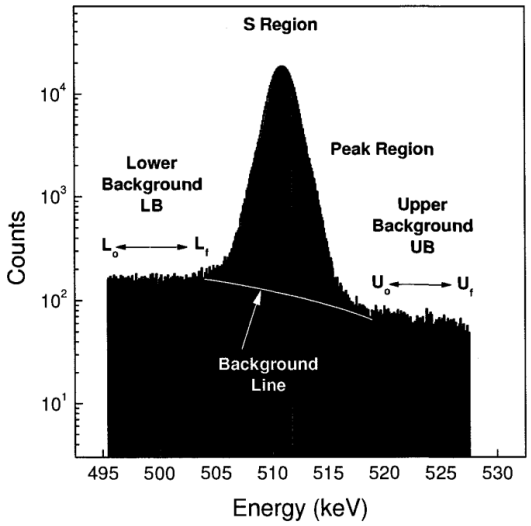

Figure 2.3 Doppler-broadened peak depicting the background line and indicating S Region and Peak Region (P_o and P_f), the Lower Background (L_o to L_f), and Upper Background (U_o to U_f) [3].

The uncertainty in the S Parameter is defined as:

$$\Delta S = \sqrt{\sum_{j=P_o}^{P_f} (\frac{dS}{dy_j}\Delta y_j)^2 + (\frac{dS}{db_l}\Delta b_l)^2 + (\frac{dS}{db_u}\Delta b_u)^2}$$

.

Data processing was performed using custom Python program called PAPPy that imported the spectrum files exported from ProSpect. Data was acquired multiple times and S parameters were computed for each sample before and after annealing. Consistency across repeated measurements was later analyzed to confirm the reproducibility of the detector setup and the stability of its calibration.

2.4 Detector Compatibility and Optimization

Software challenges also arose with the university's PAPPy data analysis environment, which exhibited incompatibilities between the ProSpect files of each detector. This is due to the inherit differences in energy to channel correlation i.e. the channel where 511 keV were different for each detector and thus the curves did not overlap and could possibly have scaling differences. This is why a reference sample is used to choose the bounds and stay consistent through all sample data measured with each detector.

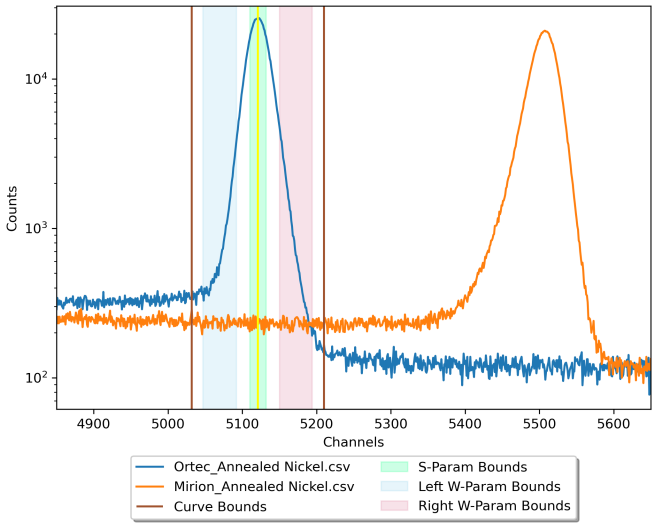

Figure 2.4 Offset 511 keV peaks measured with the Ortec detector (centered) and Mirion (right). The program shows horizontal axis to be energy, while in actuality is based on channels.

As a result, the raw data files were processed separately and using a separate reference sample for each detector and analyzed manually in the PAPPy program. Although less automated, this approach allowed direct verification of counts in the S parameter windows and ensured consistent area integration. These optimizations and corrections ultimately led to the successful qualification of the Mirion HPGe detector for precision PAS research and illuminated possible changes to the way reference samples are chosen.

Since the measurement of S Parameter is arbitrary and depends on the reference sample chosen for the bounds, we tested the linearity of the correlation between pre- and post-annealed materials for each detector as shown in the figure below (Figure 2.5).

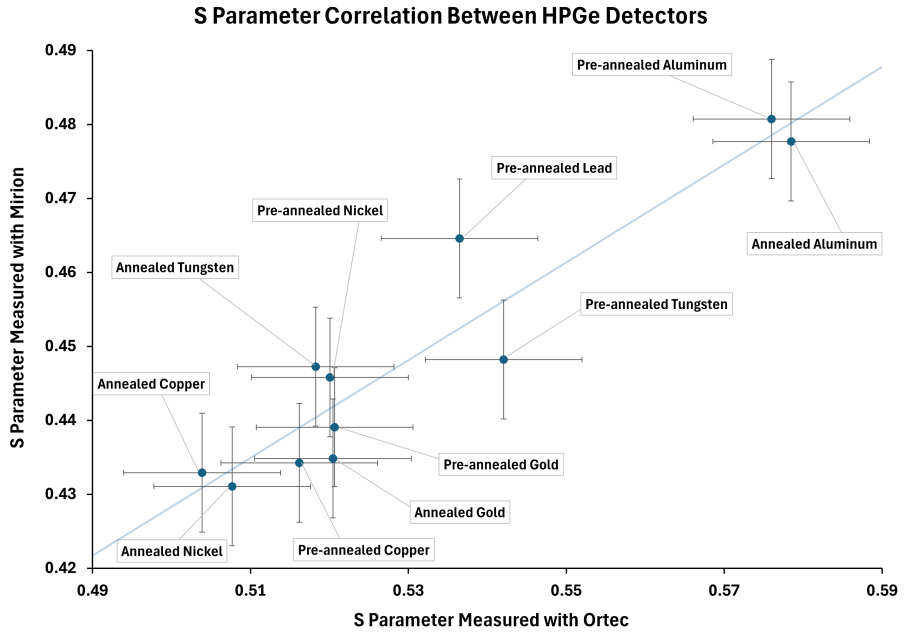

Figure 2.5 Average S Parameters for each sample measured on each detector compared. Horizontal axis (S Parameters measured on the Ortec detector), vertical axis (S Parameters measured on the Mirion detector). A linear fit line is shown ($y = 0.66x + 0.10$).

As shown, the linear relationship is not strong but present. The large error bars were due to system error from putting away samples to measure others and at later times pulling them back out. This means the sample would not be placed exactly in the same location, regardless of ensuring dead time is between 9% and 11%. The error accounted for with PAPPy is the counting error, this is for when the measurement is continually taken with no movement to the sample. This could mean a different method of calculating S Parameters might need to be implemented, by using a new reference sample each time.

Chapter 3

Results and Conclusions

3.1 Detector Qualification and Verified Results

The qualification of the newly acquired Mirion Canberra HPGe detector was successfully completed, confirming that the system performs according to the manufacturer specifications. The verification process involved assessing the energy calibration, linearity between S Parameter changes pre- and post- annealing of materials, and energy resolution through a series of controlled measurements using reference isotopes. The primary metrics used to evaluate the detector were the FWHM to determine resolution and the linearity.

Following optimization of calibration, filter settings, and pulse shaping parameters, the measured FWHM values (0.60 keV at 122 keV and 1.62 keV at 1332 keV) were comfortably within the manufacturer's guaranteed limits of $\leq$ 0.650 keV and $\leq$ 1.800 keV, respectively. These results demonstrate proper detector operation.

Table 3.1 Energy resolution (FWHM) of the Mirion Canberra HPGe detector.

Source	Energy (keV)	Measured FWHM (keV)	Specification (keV)
^{57}Co	122	0.60 ±0.0	≤ 0.650
^{60}Co	1332	1.62 ±0.02	≤ 1.800

This verified resolution is particularly significant for positron annihilation studies. Where spotting subtle variations around the 511 keV peak is critical. A detector with poorer resolution would smear fine energy differences and have louder background, obscuring Doppler broadening curves. This HPGe system ensures that future Doppler broadening spectra can be interpreted confidently in materials structure analysis.

3.2 Criteria for Detector Qualification and Analysis Reliability

Determining that the HPGe detector met the qualification criteria required not only measuring FWHM but also confirming reproducibility under repeated acquisition. Energy calibration was validated through a least-squares fit across multiple gamma-ray lines (80–1332 keV), confirming that the energy and channel relationship remained linear. A fine calibration could be implemented on a more regular basis to ensure accuracy.

There are many outer environmental things that can affect measurements as well, namely location of sample, but include temperature, nearby electric devices, vibrations, and possibly more.

Furthermore, a comparison of S parameter values calculated from multiple runs of the same sample untouched showed hardly any variation, ranging from $4.97 \cdot 10^{-4}$ to

$5.60 \cdot 10^{-4}$, demonstrating that the integrated signal analysis process was repeatable and minimal effects from counting statistics or minor environmental changes.

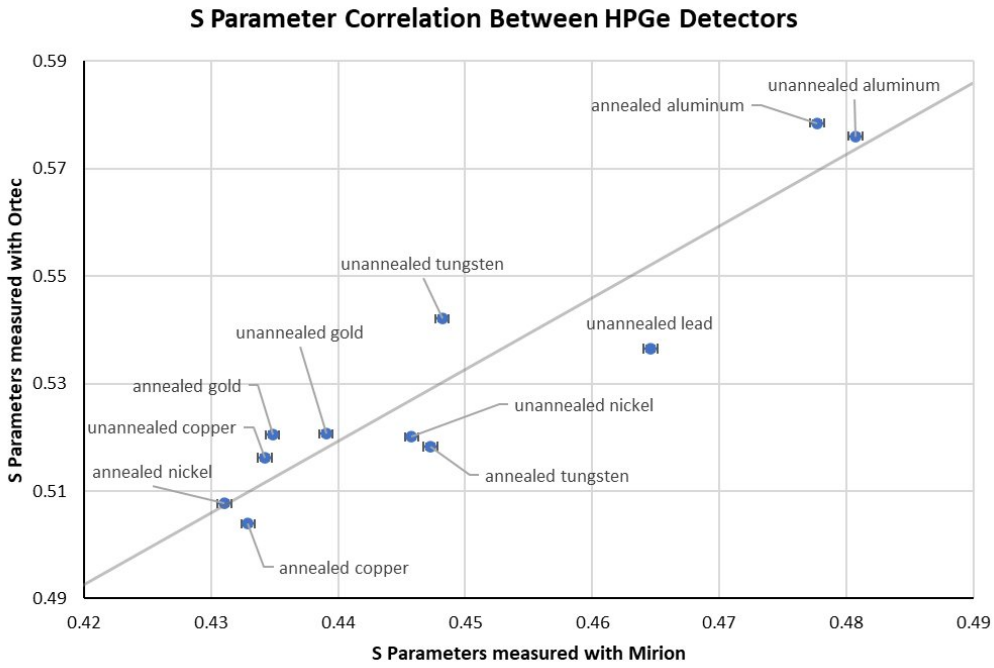

Figure 3.1 S Parameters of the same sample untouched taken multiple times with each detector. Error bar size ranges from $4.97 \cdot 10^{-4}$ to $5.60 \cdot 10^{-4}$

The proportional relationship between the S-parameter and defect density observed in previous studies [3, 7, 8] was reproduced qualitatively in test samples on the new detector, reinforcing confidence in the system's calibration and data acquisition methods. The HPGe detector thus meets all performance and reproducibility benchmarks necessary for quantitative positron annihilation research.

3.3 Future Research and Applications

The successful qualification of the HPGe detector establishes a foundation for its integration with existing positron annihilation systems of Brigham Young University

Idaho and for expanding the scope of defect characterization studies. The immediate next step involves coupling the HPGe detector with the laboratory's photomultiplier tube (PMT)-based positron lifetime spectroscopy (PLS) setup. While the PMT arrangement is already operational for timing measurements, it has not yet been used with the HPGe detectors. Integration of the two systems will allow simultaneous acquisition of lifetime and energy information from the same annihilation events, combining temporal and spectral resolution in a single experimental framework.

In the short term, this integration will focus on developing reliable coincidence timing between the PMT start signal and HPGe stop signal.This configuration would enable Coincidence Doppler Broadening (CDB) measurements in which both 511 keV photons are detected in temporal correlation. Achieving such coincidence conditions will substantially improve resolution by eliminating uncorrelated background events and allowing direct comparison of opposite photon energy shifts. The HPGe detectors' sub-keV energy resolution, combined with the nanosecond timing precision of PMTs, will create a powerful dual-mode system suitable for advanced materials research [8].

Once the HPGe and PMT hybrid setup is fully implemented, it will open multiple avenues for quantitative defect analysis. For example, combining lifetime and Doppler broadening data enables separation of vacancy size (lifetime-sensitive) from local chemical environment (momentum-sensitive). In irradiated or annealed metals, this approach can distinguish between different sized vacancies with better confidence [3, 7]. Beyond PAS, the calibrated HPGe system will remain a versatile tool for gamma-ray and X-ray spectroscopy, source standardization, and detector-response studies. Thus, the ongoing integration effort will not only enhance positron annihilation research, but also expand the laboratory's broader experimental capabilities.

Bibliography

[1] Kevin Laughlin. More efficient data collection with positron annihilation spectroscopy. Bachelor's thesis, Brigham Young University - Idaho.

[2] Mirion Technologies (CANBERRA). Detector specification and performance data for model be3830p, serial number 13936. Internal performance datasheet, aug 2023. Document DPF-009, Rev. H.

[3] Marcus A Gagliardi. *Positron defect mapping*. PhD thesis, 2008.

[4] Glenn F Knoll. *Radiation detection and measurement*. John Wiley & Sons, 2010.

[5] Mirion Technologies. Germanium detectors data sheet. https://assets-mirion.mirion.com/prod-20220822/cms4_mirion/files/pdf/spec-sheets/germanium-detectors-data-sheet.pdf, 2025. SPC-659-EN-A, March 2025. Accessed: October 01, 2025.

[6] Mirion Technologies, Inc. Bege broad energy germanium detectors specification sheet, October 2025. Document SPC-134-EN-C.

[7] Dallin Pincock. Positron annihilation and the w-parameter. Bachelor's thesis, Brigham Young University - Idaho, 2012.

[8] Joseph M. Watkins Xunxiang Hu Yasuhisa Oya Chase N. Taylor, Masashi Shimada. Neutron irradiated tungsten bulk defect characterization by positron annihilation spectroscopy. *Nuclear Materials and Energy*, 2021.

[9] Inc. Canberra Industries. *ProSpect Gamma Spectroscopy Software User's Manual*, 2012.